



$$\begin{bmatrix} i_0 \\ i_d \\ i_q \end{bmatrix} = \sqrt{\frac{2}{3}} \begin{bmatrix} \frac{1}{\sqrt{2}} & \frac{1}{\sqrt{2}} & \frac{1}{\sqrt{2}} \\ 1 & -\frac{1}{2} & -\frac{1}{2} \\ 0 & \frac{\sqrt{3}}{2} & \frac{\sqrt{3}}{2} \end{bmatrix} \begin{bmatrix} i_{s,a} \\ i_{s,b} \\ i_{s,c} \end{bmatrix} \quad (2)$$

Active and reactive components are obtained by the give relation in equation-3. Where Active and reactive components are function of load current and phase voltages.

$$\begin{bmatrix} P \\ Q \end{bmatrix} = \begin{bmatrix} v_d & v_q \\ -v_q & v_d \end{bmatrix} \begin{bmatrix} i_d \\ i_q \end{bmatrix} \quad (3)$$

$$P_0 = V_0 * I_0 \quad (4)$$

$$P = \bar{P} + \bar{P} \quad (5)$$

$$\begin{bmatrix} I_{cd,ref} \\ I_{cq,ref} \end{bmatrix} = \frac{1}{V_\alpha^2 + V_\beta^2} \begin{bmatrix} V_\alpha & -V_\beta \\ V_\beta & V_\alpha \end{bmatrix} \begin{bmatrix} -\bar{P} + P_0 + \bar{P}_{loss} \\ -Q \end{bmatrix} \quad (6)$$

$I_{cd,ref}$ , and  $i_{cq,ref}$  are extension currents of shunt APF in d-q coordinates. These current are changed to 3-- system described in equation-(7).

$$\begin{bmatrix} i_0 \\ i_d \\ i_q \end{bmatrix} = \sqrt{\frac{2}{3}} \begin{bmatrix} 1 & 0 \\ -\frac{1}{2} & \frac{\sqrt{3}}{2} \\ -\frac{1}{2} & -\frac{\sqrt{3}}{2} \end{bmatrix} \begin{bmatrix} i_{cd,ref} \\ i_{cq,ref} \end{bmatrix} \quad (7)$$

The reference current in 3-- system ( $I_{ca,ref}$ ,  $I_{cb,ref}$ ,  $I_{cc,ref}$ ) are measured in order to alter neutral, harmonic and reactive current at the load. Hysteresis band current control algorithm[12] is used to generate switching signal by comparing actual signal with reference signal, depending on speed and accuracy of reference signal the performance of UPQC can be improved.

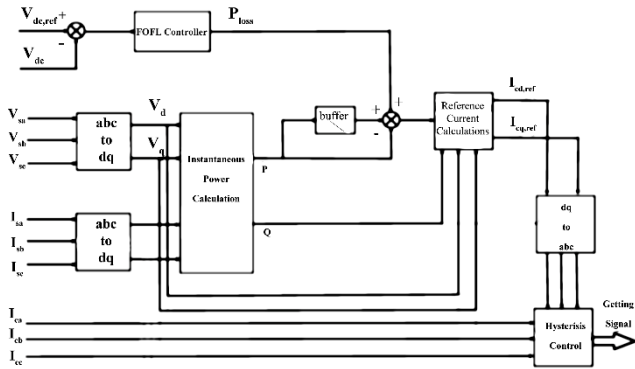


Fig. 3. Shunt APF Configuration.

## II. DESIGN OF FRACTIONAL ORDER CONTROL

Sondhi et.al.(2014) introduced the FOPI controller in[13].It is significant to understand the fractional order derivative operator. Once the fractional speculator was numerically formed. The numerical expression for FOPI is

$$c(s) = k_p + \frac{k_i}{s^\lambda} \quad (8)$$

Where  $\lambda$  can accept some value in the range (0, 1). If  $\lambda \geq 2$  the mechanism is changed to a high-order construction which is

different ability in equivalence to formal PI controller. The F.O is described in (8) may be regarded as the common character of the formal PI controller.

## III. DESIGN OF FILTER USING FRACTIONAL ORDER CONTROLLER

Molina et.al.(2006) presented the evolution of FOC, there appeared various definitions of FOD's and FOI's[12]. Online practical FOD may be needed in control systems. Using filters is one in all the most effective ways in which to solve the issues. Some consecutive filters are summarized in[13]. Assuming the expected fitting range is  $(\omega_b, \omega_h)$ , the fractional order function  $\lambda$  can be approximated by FOF(fractional order filter) can be written as,

$$K(s) = \left( \frac{1 + \frac{bs}{d\omega_b}}{1 + \frac{ds}{d\omega_h}} \right)^\lambda \quad (9)$$

Where  $0 < \lambda < 1, s = j\omega, b > 0, d > 0$ , and

$$K(s) = \left( \frac{bs}{d\omega_h} \right)^\lambda \left( 1 + \frac{-ds+d}{ds^2+b\omega_h s} \right)^\lambda \quad (10)$$

In the frequency range between  $\omega_b < \omega < \omega_h$ , by using a Taylor polynomial expansion, it acquires

$$K(s) = \left( \frac{bs}{d\omega_h} \right)^\lambda \left( 1 + \lambda P(s) + \frac{\lambda(\lambda-1)}{2} P^2(s) \dots \right) \quad (11)$$

$$\text{Where } p(s) = \frac{-ds^2+d}{ds^2+b\omega_h s} \quad (12)$$

It is initiate that

$$s^\lambda = \frac{(d\omega_b)^\lambda b^{-\lambda}}{\left[ 1 + \lambda P(s) + \frac{\lambda(\lambda-1)}{2} P^2(s) \dots \right]} \left( \frac{1 + \frac{bs}{d\omega_b}}{1 + \frac{ds}{d\omega_h}} \right)^\lambda \quad (13)$$

Estimated the Taylor polynomial to leads to

$$s^\lambda \approx \frac{(d\omega_b)^\lambda}{b^\lambda [1 + \lambda P(s)]} \left( \frac{1 + \frac{bs}{d\omega_b}}{1 + \frac{ds}{d\omega_h}} \right)^\lambda \quad (14)$$

Thus, the FOD is defined as

$$s^\lambda \approx \left( \frac{d\omega_b}{b} \right)^\lambda \left( \frac{ds^2+b\omega_h s}{d(1-\lambda)s^2+b\omega_h s+d\lambda} \right)^\lambda \left( \frac{1 + \frac{bs}{d\omega_b}}{1 + \frac{ds}{d\omega_h}} \right)^\lambda \quad (15)$$

Equation (15) is balanced if and only if all the poles are LHS of the complex s-plane. The poles of the above expression is

$$d(1-\lambda)s^2 + b\omega_h s + d\lambda \quad (16)$$

The negative poles in real part for  $0 < \lambda < 1$ . thus, all thepoles of (15) are within the range of  $(\omega_l, \omega_h)$ .The magnitude relation fractional-order part of formulation (14) can be approximated by the uninterrupted-time coherent simulation.

$$K(s) = \lim_{N \rightarrow \infty} k_N(s) = \lim_{N \rightarrow \infty} \prod_{k=1}^N \frac{1 + \frac{s}{\omega_k}}{1 + \frac{s}{\omega_k}} = -N \frac{1 + \frac{s}{\omega_k}}{1 + \frac{s}{\omega_k}} \quad (17)$$

accordant to the algorithmic distribution of actual zeros and poles, the rank  $k$  can be written as

$$\omega'_k = \left(\frac{d\omega_b}{b}\right)^{\frac{\lambda-2k}{2N+1}}, \omega_k = \left(\frac{d\omega_h}{b}\right)^{\frac{\lambda+2k}{2N+1}} \quad (18)$$

Thus, the continual coherent transfer function representation can be written as

$$s^\lambda \approx \left(\frac{d\omega_b}{b}\right)^\lambda \left(\frac{ds^2 + b\omega_n^5}{d(1-\lambda)s^2 + b\omega_n s + d\lambda}\right) \prod_{k=1}^N \frac{s + \omega'_k}{s + \omega_k} \quad (19)$$

Direct confirmation by enquiry and theoretical analysis, this

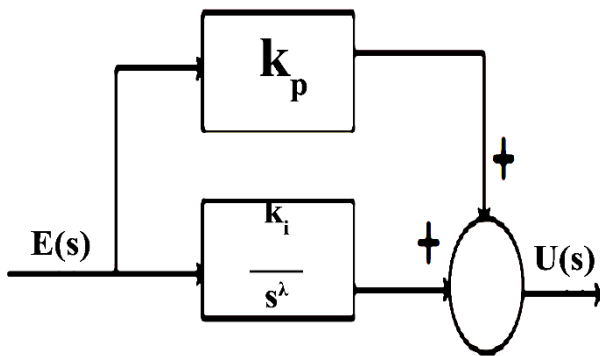


Fig. 4. Structure of FOPI controller.

analysis similarity can prevail the good essence when  $b = 12$  and  $d = 10$ . Though the estimation method, the FOS may be approximated as the very eminent integer-order system. A fractional-order integration can be obtain changing the sign of order ( $\lambda$ ). Hence, the range of  $\lambda$  for integration is  $0 < \lambda < 1$ . The structure of FOPI controller is shown in Fig. 4. for design a controller the  $K_p$  element,  $\lambda$  are individually designed and place in the structure show in Fig. 4.

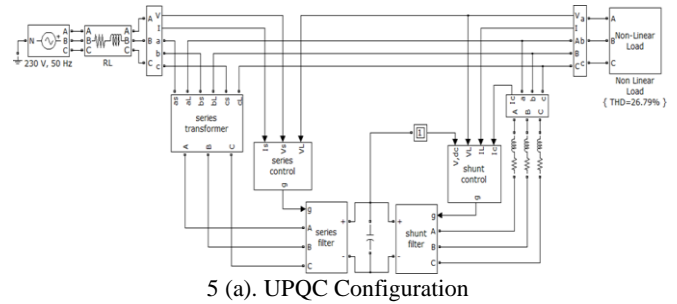
#### IV. SIMULATION RESULTS

Simulations are performed using MATLAB-SIMULINK. The parameters used to simulate UPQC are given in Table-I.

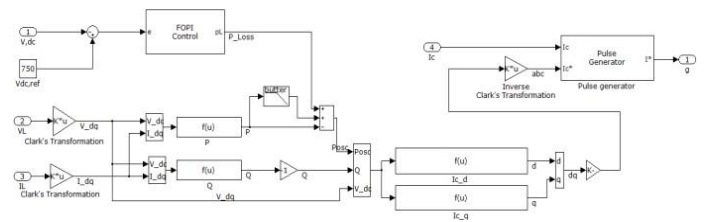
Table-1: UPQC system parameters

System Parameters		
Supply voltages	$V_{s,abc} L-L$	380 V
Supply Frequency	$f_s$	50Hz
DC-link voltage	$V_{dc}$	750V
Load	$R_L, L_L$	20 $\Omega$ , 15mH
Series active power filter parameters		
Series transformer	Rate	1/3
AC filter	$R_f, C_f$	5 $\Omega$ , 3 $\mu F$
AC inductance	$L_c$	3.5mH
Shunt active power filter parameters		
AC inductance	$L_f$	1mH

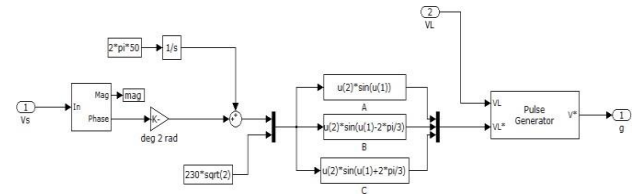
DC resistance	$R_d$	100 $\Omega$
DC inductance	$L_d$	10mH
DC capacitor	$C_{DC}$	2000 $\mu F$



5 (a). UPQC Configuration



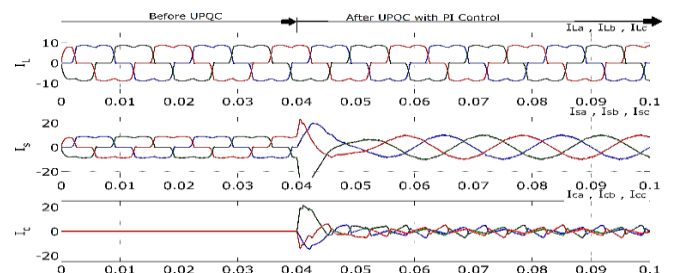
5 (b). Shunt Control block



5 (c). Series Control block

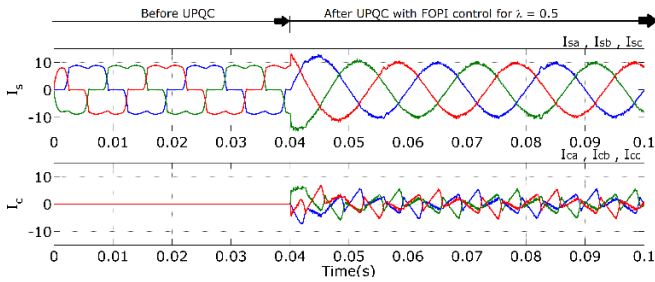
#### A. Voltage and current harmonics Compensation

In the conventional and proposed control algorithm, the simulation results load current ( $I_{Labc}$ ), source current ( $I_{Sabc}$ ), and compensating current ( $I_{Cabc}$ ) waveforms are shown in Fig. 6 before and after the UPQC is operation with PI control and FOPI control for  $\lambda=0.5$ . Fig. 7 shows the simulation results for load voltage harmonics mitigation with UPQC based PI and FOPI controller when introduction of 5<sup>th</sup> (20%) and 7<sup>th</sup> (14%) order voltage at 0.2 sec for a duration of 0.2 sec into the source voltage as shown in Fig. 7(a). The series APF injects an out-of-phase voltage with 5<sup>th</sup> and 7<sup>th</sup> harmonics which is difference between the desired load voltage and actual supply.



6 (a). With UPQC based PI control





6. (b). With UPQC based FOPI control for  $\lambda=0.5$  Fig. 8. Load, source and compensating current before and after UPQC operation.

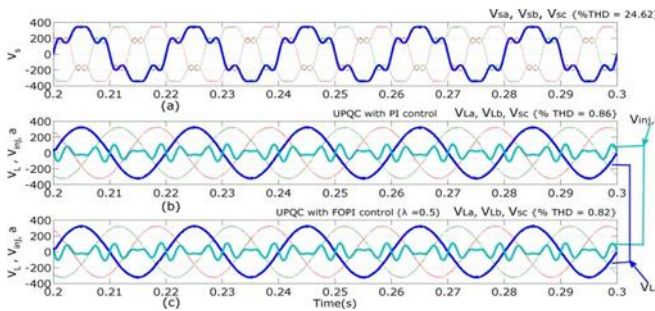


Fig. 7. Mitigation of load voltage harmonics with UPQC based PI control and FOPI control

Simultaneously, shunt APF with PI control and FOPI control regulates the dc-link voltage to the reference dc-link voltage as shown Fig. 8.

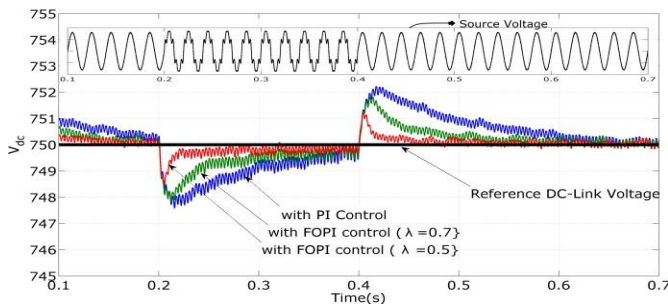


Fig. 8. Regulation of DC-Link voltage for harmonics in source voltage

## B. Voltage sag and current harmonic mitigation

The simulation results of voltage sag and current harmonics mitigation for UPQC based PI control and FOPI control is observed in Fig.9 and 10 respectively.

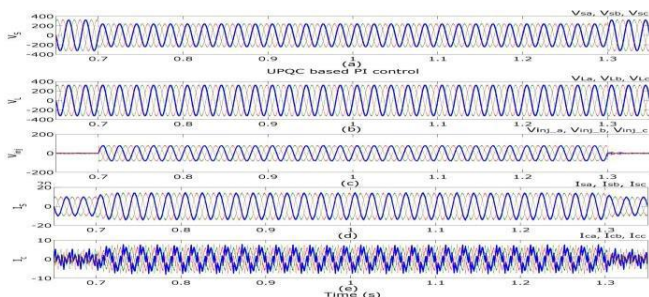


Fig. 9 Mitigation of Load voltage sag and current compensation by UPQC based FOPI control.

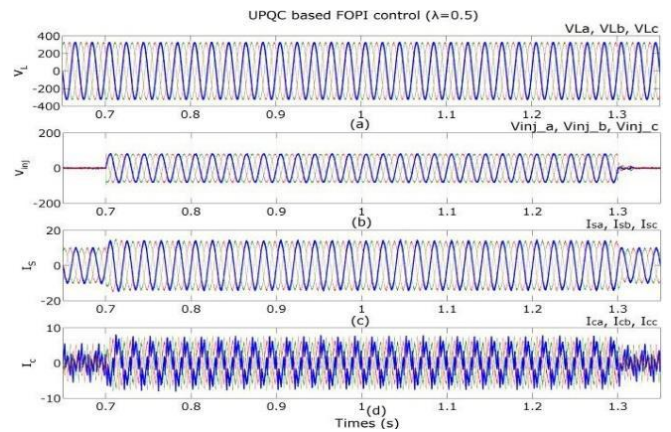


Fig. 10 Mitigation of Load voltage sag and current compensation by UPQC based FOPI control.

in order to keep this DC link voltage at fixed level as shown in Fig. 11. If it is not well-maintained, the DC link voltage will inject to very low value and UPQC fails.

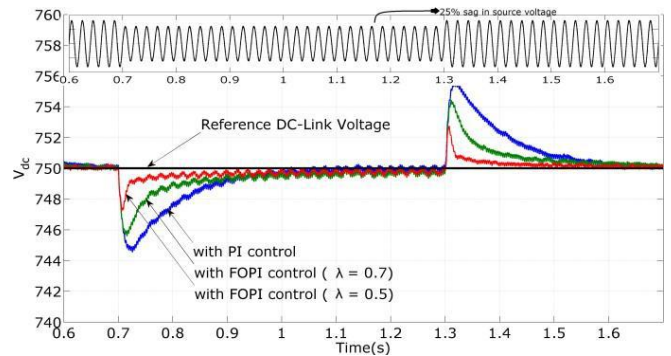


Fig. 11. Regulation of DC-Link voltage for Voltage sag

## C. Voltage swell and current harmonics mitigation.

The simulation results of voltage swell reduced by UPQC based PI control and FOPI control is shown in Fig. 12 and Fig. 13 respectively.

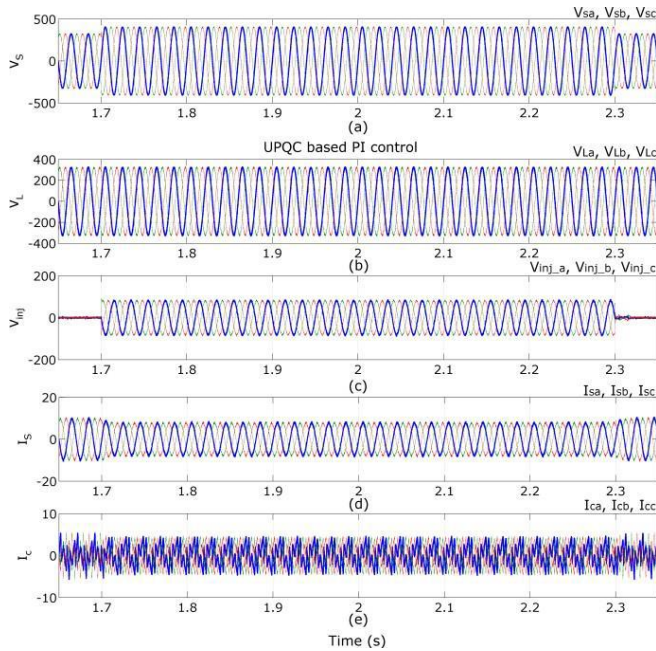


Fig. 12 Mitigation of Load voltage swell and current compensation by UPQC based PI control

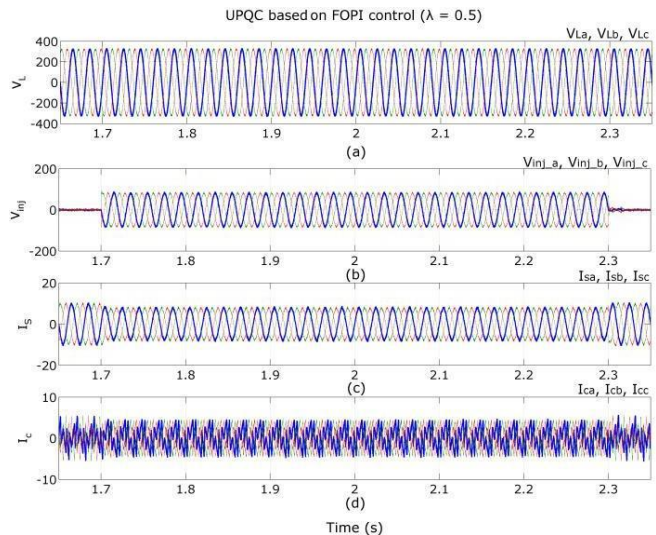


Fig. 13 Mitigation of Load voltage swell and current compensation by UPQC based FOPI control

At the same time, increasing in source voltage consequences in the rise in DC-link voltage and is regulated by shunt APF by respective controller as shown in Fig. 14.

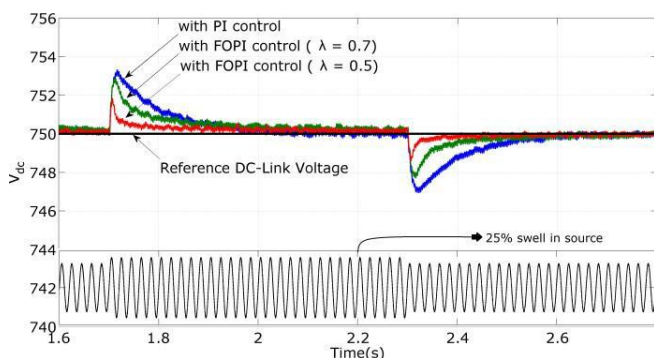


Fig. 14 Regulation of DC-Link voltage for Voltage swell  
From Fig. 8, 11 and 14, it is observed that the FOPI

controller regulates the dc-link voltage faster than PI control which shows that proposed controller calculates the reference current more efficiently and quickly than conventional controller. Table II gives the harmonic comparison of UPQC based FOPI controller with UPQC based PI controller. Here, Load current is constant throughout the simulation for all controllers with %THD = 25.68. From Table II, the performance is found to be in close approximation with that of the PI controller; however, there is considerable improvement can be observed which shows the FOPI controller has good performance with the extra parameter included into the controller.

Table II

Comparison of %THD in voltage and current for UPQC based PI and FOPI controller.

	PI control	FOPI $\lambda = 1.1$	FOPI $\lambda = 0.7$	FOPI $\lambda = 0.5$
Source voltage contain harmonics (%THD = 24.64)				
Load Voltage	0.86	0.89	0.86	0.82
Source current	2.70	2.48	2.47	2.17
25% sag in Source voltage				
Load Voltage	0.56	0.59	0.55	0.55
Source current	1.60	1.83	1.60	1.57
25% swell in Source voltage				
Load Voltage	0.6	0.66	0.6	0.6
Source current	2.60	2.71	2.52	2.52

#### IV. CONCLUSION

In this proposed work a FOPI based UPQC is proposed to mitigate the well-known power quality issues, popularly known as harmonic compensation and load voltage sag. The performance of UPQC is demonstrated on power distribution system consisting of nonlinear loads. The UPQC with FOPI controller is quite capable of mitigating power quality issues compared to UPQC with PI controller.

#### REFERENCES

1. B. Singh, A. Adya, A. Mittal, and J. Gupta, "Power quality enhancement with DSTATCOM for small isolated alternator feeding distribution system," in *2005 International Conference on Power Electronics and Drives Systems*, 2005, vol. 1, pp. 274-279: IEEE.
2. D. Nair, M. Raveendran, A. Nambiar, N. P. Mohan, and S. Sampath, "Mitigation of power quality issues using DSTATCOM," in *2012 International Conference on Emerging Trends in Electrical Engineering and Energy Management (ICETEEEM)*, 2012, pp. 65-69: IEEE.
3. G. O. Suvire and P. E. Mercado, "Improvement of power quality in wind energy applications using a DSTATCOM coupled with a flywheel energy storage system," in *2009 Brazilian Power Electronics Conference*, 2009, pp. 58-64: IEEE.
4. T. Zaveri, B. Bhavesh, and N. Zaveri, "Control techniques for power quality improvement in delta connected load using DSTATCOM," in *2011 IEEE International Electric Machines & Drives*

- Conference (IEMDC)*, 2011, pp. 1397-1402: IEEE.
5. K.-H. Kuypers, R. Morrison, and S. Tennakoon, "Power quality implications associated with a series FACTS controller," in *Ninth International Conference on Harmonics and Quality of Power. Proceedings (Cat. No. 00EX441)*, 2000, vol. 1, pp. 176-181: IEEE.
  6. O. G. Ibe and A. I. Onyema, "Concepts of reactive power control and voltage stability methods in power system network," *IOSR Journal of Computer Engineering*, vol. 11, no. 2, pp. 15-25, 2013.
  7. A. Ghosh and G. Ledwich, *Power quality enhancement using custom power devices*. Springer Science & Business Media, 2012.
  8. S.-M. Woo, D.-W. Kang, W.-C. Lee, and D.-S. Hyun, "The distribution STATCOM for reducing the effect of voltage sag and swell," in *IECON'01. 27th Annual Conference of the IEEE Industrial Electronics Society (Cat. No. 37243)*, 2001, vol. 2, pp. 1132-1137: IEEE.
  9. M. Molina and P. Mercado, "Control design and simulation of DSTATCOM with energy storage for power quality improvements," in *2006 IEEE/PES Transmission & Distribution Conference and Exposition: Latin America*, 2006, pp. 1-7: IEEE.
  10. Y. Wang, J. Li, Y. Lv, and X. Liu, "Modeling and Controller design of distribution static synchronous compensator," in *2006 International Conference on Power System Technology*, 2006, pp. 1-5: IEEE.
  11. V. Virulkar and M. Aware, "Analysis of DSTATCOM with BESS for mitigation of flicker," in *2009 International Conference on Control, Automation, Communication and Energy Conservation*, 2009, pp. 1-7: IEEE.
  12. B. P. Muni, S. E. Rao, and J. Vithal, "SVPWM switched DSTATCOM for power factor and voltage sag compensation," in *2006 International Conference on Power Electronic, Drives and Energy Systems*, 2006, pp. 1-6: IEEE.
  13. A. Wächter and L. T. Biegler, "On the implementation of an interior-point filter line-search algorithm for large-scale nonlinear programming," *Mathematical programming*, vol. 106, no. 1, pp. 25-57, 2006.